Dissecting the Role of G-protein Signalling on Primary Metabolism in the Wheat Pathogen *Stagonospora nodorum*

Joel P.A. Gummer[1,2], Robert D. Trengove[1,2], Richard P. Oliver[3] and Peter S. Solomon[4]*

1 Separation Science and Metabolomics Laboratory, Murdoch University, Perth 6150, WA, Australia, **2** Metabolomics Australia, Murdoch University, Perth 6150, WA, Australia, **3** Australian Centre for Necrotrophic Fungal Pathogens, Department of Environment and Agriculture, Curtin University, Perth 6102, WA Australia, **4** Division of Plant Sciences, Research School of Biology, The Australian National University, ACT 0200, Australia.

Correspondence: Peter S. Solomon, peter.solomon@anu.edu.au, +61-2-6125-3952

Main text word count: 5711

Summary word count: 200

Figures: 5, **Tables**: 4

Running title: G-protein signalling in *Stagonospora nodorum*

Contents category: Physiology and Biochemistry

Summary

Mutants of the wheat pathogenic fungus *Stagonospora nodorum* lacking G-protein subunits display a variety of phenotypes including melanisation defects, primary metabolic changes and a decreased ability to sporulate. To better understand the causes of these phenotypes, *Stagonospora nodorum* strains lacking a Gα, Gβ or a Gγ subunit were compared to a wild-type strain using metabolomics. Agar plate growth at 22°C revealed a number of fundamental metabolic changes and highlighted the influential role of these proteins in glucose utilisation. A further characterisation of the mutants was undertaken during prolonged storage at 4°C; conditions known to induce sporulation in these sporulation-deficient signalling mutants. The abundance of several compounds positively correlated with the onset of sporulation including the dissacharide trehalose, the tryptophan degradation product tryptamine and the secondary metabolite alternariol; metabolites all previously associated with sporulation. Several other compounds decreased or were absent during sporulation. The levels of one such compound, (Unknown_35.27_2194_319), decreased from being one of the more abundant compounds to absence during pycnidial maturation. This study has shed light on the role of G-protein subunits on primary metabolism during vegetative growth and exploited the cold-induced sporulation phenomomen in these mutants to identify some key metabolic changes that occur during asexual reproduction.

INTRODUCTION

Stagonospora nodorum is a filamentous fungus and the causal agent of stagonospora nodorum blotch (SNB) on wheat (Solomon *et al.*, 2006a). It is a necrotrophic pathogen that relies on the secretion of small, secreted proteinaceous effectors to cause disease in an inverse gene-for-gene manner (Oliver & Solomon, 2010). Recent reverse genetic approaches have identified many genes, proteins, pathways and metabolites that play important roles in enabling *S. nodorum* to complete its pathogenic lifecycle (Oliver *et al.*, 2012).

One aspect of the disease that has received considerable attention has been signal transduction, and in particular, cAMP-dependent signalling. Mutants of *S. nodorum* harbouring inactive copies of a Gα (*Gna1*, Gα I class), a Gβ (*Gba1*) or a Gγ (*Gga1*) subunit were all only weakly pathogenic at best and displayed a number of other phenotypes *in vitro* including nitrogen utilisation deficiencies, impaired melanisation and a decrease in extracellular protease activity (Gummer *et al.*, 2012; Solomon *et al.*, 2004). Another phenotype common to mutants lacking either of the heterotrimeric G-protein subunits listed above was a complete lack of sporulation, either *in vitro* or *in planta*. A recent study though by Gummer *et al* (2012) described how prolonged storage at 4°C could induce sporulation in all of the mutants. After incubation at 4°C for six weeks, pycnidia appeared containing viable pycnidiospores whilst no pycnidia differentiated after incubation at 22°C for an equivalent time. The mechanism behind the cold-induced sporulation is unknown.

Proteomics approaches have been exploited to better understand the role of these signalling genes in disease and fungal development (Bringans *et al.*, 2009; Casey *et al.*, 2010; Tan *et al.*, 2009a). Conventional two-dimensional gel approaches along with

quantitative liquid chromatography methods have identified several targets regulated by these G-protein subunits in *S. nodorum*. For example, a comparative proteomic analysis of the *gna1-35* strain identified that the Sch1 protein was positively regulated by Gα signalling (Tan *et al.*, 2008). Subsequent analysis of the *S. nodorum sch1* mutant strain revealed the massive accumulation of the mycotoxin alternariol. This was the first such identification of a mycotoxin in *S. nodorum* and highlighted the potential human health impact of SNB disease (Tan *et al.*, 2009b).

A complementary approach to study these mutants is metabolomics. Metabolomics is a non-targeted method to relatively quantitate the metabolites present in a given sample at the time of sample harvest (Gummer *et al.*, 2011; Kim *et al.*, 2011). Metabolomics is an appropriate method with which to understand how cold storage triggers asexual sporulation as several studies in *S. nodorum* to date have highlighted the importance of primary metabolites in differentiation.

One such study identified that mannitol metabolism exists as two separate pathways, rather than the previously hypothesized single cycle (Solomon *et al.*, 2005; Solomon *et al.*, 2006c; Solomon *et al.*, 2007). These studies showed that the inability of a *S. nodorum* mutant to sporulate was correlated with the depletion of the intracellular mannitol pool. Studies of the *mpd1* mutant strain, compromised in its ability to synthesise or grow on mannitol as a sole carbon source, established mannitol as playing an essential role in asexual sporulation in *S. nodorum* both *in vitro* and *in planta* (Solomon *et al.*, 2006c). Interestingly in the mannitol-depleted strain, the reduced intensity of mannitol in metabolite profiles appeared to be compensated by an increased abundance of trehalose.

In a separate study by Lowe *et al*., trehalose abundance was also linked to asexual sporulation in *S. nodorum* (Lowe *et al.*, 2009). Trehalose synthesis was disrupted by deletion of a trehalose 6-phosphate synthase (*Tps1*) gene, with the resulting *tps1* strain possessing a reduced capacity to develop pycnidia, and failing to progress into asexual sporulation. Gas chromatography-mass spectrometry (GC-MS) analysis of metabolite extracts of the *tps*1 strain showed a correlation between trehalose abundance and asexual sporulation both *in vitro* and in wheat (Lowe *et al.*, 2009).

The phenotypes of the *S. nodorum gna1-35*, *gba1-6* and *gga1-25* strains are of considerable interest, and provided an opportunity to link specific biochemical events to signalling in *S. nodorum*. Of particular interest is the resulting phenotype of the signalling mutants during prolonged cold storage and the opportunity they provide to further dissect asexual sporulation in *S. nodorum*. In this study, an untargeted metabolomic analysis was used to dissect the phenotypes of *S. nodorum* wild-type strain SN15, and the changes that occurred to the metabolome as a result of the inactivated *Gna1*, *Gba1* and *Gga1* genes.

METHODS

Preparation of plate-cultured *S. nodorum* for metabolite extraction. *S. nodorum* wild-type SN15 and strains *gna1-35*, *gba1-6* and *gga1-25*, were inoculated from minimal medium (30 g l^{-1} sucrose, 2 g l^{-1} $NaNO_3^-$, 1.0 g l^{-1} K_2HPO_4, 0.5 g l^{-1} KCl, 0.5 g l^{-1} $MgSO_4 \cdot 7H_2O$, 0.01 g l^{-1} $ZnSO_4 \cdot 7H_2O$, 0.01 g l^{-1} $FeSO_4 \cdot 7H_2O$, 0.0025 g l^{-1} $CuSO_4 \cdot 5H_2O$) agar-cultured mycelia, onto the centre of a sterile nitrocellulose filter (overlayed on minimal medium agar). The composition of minimal medium has been previously described (Solomon *et al.*, 2006b). Cultures were grown with a 12-h white-light regimen at 22°C.

For the simultaneous analysis of intracellular and extracellular metabolites, cultures were grown for five, eight or 10 days, with six replicates harvested per strain at each time point. For the analysis of intracellular metabolites, cultures were grown for five or 10 days, with six cultures harvested per strain at each time point. For the analysis of intracellular metabolites under asexually sporulating conditions, cultures were grown for five days then incubated at 4°C for three or six weeks before harvesting. Six cultures were prepared per strain per time point.

Fungal cultures were harvested by scraping the mycelia from the nitrocellulose (overlaying the growth medium) using a scalpel, or by transferring the entire nitrocellulose filter into a two ml safe-lock microcentrifuge tube. Each replicate was harvested in less than 10 seconds. The samples were then dried by lyophilisation in a LABCONCO Freezone 2.5 Plus (©Labconco Corp., USA) depressurized with a JLT-10 JAVAC high vacuum pump (JAVAC Pty. Ltd., Australia).

Metabolite extraction and isolation. Metabolites were extracted from between five and 10 mg dried mycelium. Fungal mycelia were transferred to a two ml safe-lock microcentrifuge tube containing a three mm diameter ball bearing. To the tube was added 685 μl of -40°C methanol and the tube shaken vigorously in a Retsch® MM301 lyser (Retsch®, UK) at 30 (Htz; 1/s) for two minutes. 75 μl of water containing 1.25 μg ribitol (internal standard) was added to the suspension per one mg of fungal tissue and the tube returned to the tissue lyser for a further two minutes. For extractions containing nitrocellulose, the methanol and water were added together before shaking in the lyser. Following which, the tube was frozen in liquid nitrogen, and thawed on ice. After briefly mixing the suspension by vortexing,, cell debris were collected by centrifugation in an eppendorf 5415R centrifuge (eppendorf, USA) at 20,000 *g* for two minutes. The supernatant was then transferred to a fresh microcentrifuge tube. 250 μl of -40°C 90% methanol was added to the remaining pellet and the tube shaken in the lyser for two minutes. The cell debris was again collected by centrifugation at 20,000 *g* for two minutes. The supernatant was added to the previous and the pellet discarded. The combined supernatant was vortexed and a two mg-fungal-tissue equivalent volume transferred to a fresh tube and dried in preparation for chemical derivatisation by; first removing the methanol by evaporation in an eppendorf Concentrator Plus vacuum concentrator (eppendorf, USA) before then freezing the remaining extract in liquid nitrogen and drying it in a LABCONCO Freezone 2.5 Plus (©Labconco Corp., USA) depressurized with a JLT-10 JAVAC high vacuum pump (JAVAC Pty. Ltd., Australia).

MEOX-TMS derivatisation of fungal metabolites for GC-MS analysis. The dried fungal metabolites were derivatised by a combination of oximation and silylation reactions. To the dried metabolite extract was added 20 μl of methoxylamine HCl (Sigma-Aldrich, Australia) [20mg/ml in pyridine (©UNIVAR)], followed by a brief vortex to mix and incubation in an eppendorf Thermomixer (Eppendorf, USA) at 30°C for two hours with shaking at 1250 *rpm*. 40 μl MSTFA (©Thermo Fisher Scientific Inc., USA) was then added, vortexed briefly to mix, and incubated at 37°C for one hour whilst shaking at 1250 *rpm*. The derivatised product was then transferred to a 200 μl glass vial insert within a 1.5 ml amber vial (Grace Davison Discovery Sciences, Australia) and five μl of a mixture of alkanes (Retention index standard) added and mixed. The solution was then sealed within the vial with an 11 mm aluminium crimp cap seal (Grace Davison Discovery Sciences, Australia).

GC-MS analysis of fungal metabolite extracts. Derivatized metabolites (1 µl) were injected into a split/splitless GC inlet using a 20:1 split injection mode, for GC-MS analysis. The GC-MS equipment consisted of an Agilent 7680 autosampler, an Agilent 6890 gas chromatograph, and an Agilent 5973N quadrupole mass spectrometer (©Agilent, Palo Alto, CA, USA). The GC-MS system was autotuned using perfluorotributylamine (PFTBA). A 30-m Varian VF-5ms FactorFour column with a 10-m integrated Varian EZ-Guard column was used (Varian, Palo Alto, CA, USA). The injection inlet temperature was 230°C, with an interface temperature of 300°C, and an ion source temperature of 230°C. Helium was used as the carrier gas, and the flow rate was retention time locked to elute a derivatised mannitol standard at RT 30.6 minutes using the Chemstation (©Agilent, Palo Alto, CA, USA) software. The temperature

gradient consisted of an initial temperature of 70°C, increasing at 1°C per minute for 5 min before increasing to a final hold temperature of 300°C at a temperature ramp rate of 5.6°C per minute with a transfer line temperature of 330°C.

Data processing and analysis. AnalyzerPro™ (SpectralWorks Ltd., Runcorn, United Kingdom) was used to deconvolute and library match the acquired mass spectra. Metabolite peak areas representing the abundance of the metabolites were normalized, and the data was cross-referenced against the target component library using the MatrixAnalyser add-on. Peaks that could not be matched to the target component library were described as unknown metabolites and were given a MST name labelled according to the following format: 'Unknown_retention time_retention index_base peak'. Overloaded chromatographic peaks were re-processed with the software and analytes quantified on a single ion determined not to be saturated when detected in the MS. Putative identifications were assigned to unknown metabolites using the Library Search function of AnalyzerPro™ on the deconvoluted mass spectra, and the National Institute of Standards and Technology (NIST, USA) Mass Spectral Library.

Data sets were exported from AnalyzerPro™ for calculations and layout manipulation using Microsoft Excel. 'Normalised' analyte abundances were calculated by dividing the determined analyte peak area by that determined for ribitol (internal standard). The determined analyte peak areas were then divided by the weight of the fungal tissue used in the extract.

The scripting program Ruby was used to design and implement a script for the alignment of mass spectral peaks common across the generated data sets in the Ruby programming language. The script used the outputted AnalyzerPro™ Summary Report

to align all peaks eluting within 0.05 1/100ths of a minute, identified with a common base peak (m/z). The acquired data output was integrated with the AnalyzerPro™ Matrix Analyzer output to produce the final metabolomic data set.

Metabolomic datasets were subjected to principal component analysis (PCA; The Unscrambler®, CAMO Software, AS) using a Full-Cross Validation, subsequent to scaling [$x = \log(x + 1)$] of the metabolite abundances. Figures were edited for visual purposes. Normalised metabolite abundances were analysed by Tukey Kramer analysis (JMP 8.0.2®, SAS Institute) for a determination of statistical significance.

Results

Metabolome analysis of *S. nodorum* strains SN15, *gna1-35*, *gba1* and *gga1*

The intracellular metabolomes of *S. nodorum* strains SN15, *gna1-35*, *gba1-6* and *gga1-25* were analysed at both five and 10 days post inoculation (dpi). These time points represent earlier and later stages of growth. Tables 1 and 2 display the relative abundance of the identified metabolites determined to be differentially abundant ($p < 0.05$) between at least one of *gna1-35*, *gba1-6* or *gga1-25* and the wild-type SN15. Differentially abundant unidentified metabolites are listed in Supplementary Tables 1 and 2.

At 5 dpi, many of the compounds that were differentially abundant in most or all of the mutants compared to SN15 were sugars or sugar alcohols including glucose, fructose, glucopyranose and arabitol. Other compounds of interest that differed in the wildtype compared to the mutants included ornithine and also the mycotoxin alternariol. By 10 dpi, many of the sugars were no longer significantly different between the strains. Several organic acids though, such as succinic acid, fumaric acid, α-ketoglutaric acid, malic acid and citric acid, were altered in abundance, particularly *gga1-25*, compared to SN15. It was also notable that several amino acids differed in abundance, particularly in the *gna1-35* and *gga1-25* strains.

The combined intracellular and extracellular metabolites of each of the strains were also examined. By comparing these data to the intracellular results above, we sought to identify and relatively quantitate compounds secreted in the mutants. This approach was chosen due to technical limitations impeding the direct measurement of

extracellular metabolites using the nitrocellulose filter growth system. The PCA and loading scores plots are shown in Supplementary Fig. 1 and 2.

A comparison of the normalised intracellular mannitol abundances, with those determined for the combined intracellular and extracellular metabolite analysis revealed some significant discrepancies when comparing the wild-type and the mutant strains (Fig. 1). Whilst intracellular mannitol was significantly depleted between five and 10 dpi for the wild-type SN15 and mutant strain *gba*1-6, there was an insignificant, if not opposite trend, for the combined intra/extracellular measurement of mannitol in these two strains over this time. This observation could be explained only by the presence of extracellular mannitol, and may suggest the secretion of this metabolite by some strains.

The levels of glucose also differed significantly when comparing the intracellular to the combined intra/extracellular samples between the different strains (Fig. 2). The abundance of Glucose (summed for the two chromatographic instances, 5TMS_30.21_1884_319 and 5TMS 30.39_1902_319) was determined to be 4.59, 5.00 and 3.75 times less in *gna1-35*, *gba1-6* and *gga1-25*, respectively. Glucose 5TMS_30.39_1902_319 was 4.25, 4.18 and 3.50 times less in *gna1-35*, *gba1-6* and *gga1-25*, respectively. Although less in all mutant strains, at this time, glucose remained available in high abundance in the growth medium for both wild-type and mutant strains, as was the objective of the chosen five day time point. It was also confirmed that by 10 days, both intracellular and extracellular glucose levels had dropped dramatically, in some replicates to below detection limits. At 10 dpi therefore, there was no significant difference between the amount of glucose within the mutants and wild-type.

Dissecting the cold-induced sporulation phenomenon

The metabolomic data presented thus far has identified changes that have occurred to the metabolome of *S. nodorum* as a result of the deactivation of *Gna1*, *Gba1* or *Gga1*. Under these conditions, wild-type SN15 sporulates readily, whilst the mutant strains *gna1-35*, *gba1-6* and *gga1-25* do not sporulate for at least 6 weeks. The recorded metabolite abundances therefore likely reflect both direct and indirect metabolic consequences of the mutation. In a previous study by this laboratory, we demonstrated that ongoing cold stress was sufficient to induce moderate levels of asexual sporulation in the mutant strains (Gummer *et al.*, 2012). As previous sporulation studies in *S. nodorum* have highlighted the role of primary metabolism in this developmental stage (IpCho *et al.*, 2010; Lowe *et al.*, 2009; Solomon *et al.*, 2005; Solomon *et al.*, 2006c; Tan *et al.*, 2008), metabolomics was again used to dissect the cold-induced response, and identify which metabolites are specifically associated with asexual sporulation.

Each strain was incubated for 6 weeks before harvesting the mycelia for metabolite analysis (defined as 'sporulating$^{4°C}$'). These data were compared with the non-sporulating metabolomes already measured (defined as 'non-sporulating$^{22°C}$'). To highlight some of the metabolites associated with the cold-stress response and to strengthen the argument of sporulation-linked metabolites, cultures were also harvested at another time, after just 3 weeks at 4°C (defined as 'near-sporulating$^{4°C}$').

Examination of the strains at the near-sporulating$^{4°C}$ stage confirmed the mutant strains of *S. nodorum, gna1-35*, *gba1-6* and *gga1-25* showed no visible signs of pycnidia formation, and were non-sporulating, as observed with the cultures harvested 10 dpi (ie. non-sporulating$^{22°C}$). At sporulation$^{4°C}$, each of the mutant strains differentiated mature pycnidia and viable asexual spores could be harvested as previously described

(Gummer *et al.*, 2012). Metabolites were harvested from all cultures, analysed by GC-MS and the normalised metabolite abundances for each of the strains under all conditions were modelled by PCA (Fig. 3).

The PCA Scores plot identified differences in the wild-type strain SN15, under each of the culture conditions. This was observed in the projections of both principal components one (PC1: 30%) and two (PC2: 16%). Both components also displayed the collective similarities of the chilled non-sporulating mutant strains, with the non-sporulating mutants cultured at 22°C. The latter non-sporulating strains however clustered with the sporulating mutants, and interestingly also with SN15 under the comparative sporulating culture conditions. An analysis of the PCA Loadings revealed that the scores were highly influenced by only a few metabolites. The most influential metabolites of PCs1 and 2 are displayed in Fig. 4.

Statistical differences in metabolite abundances between each of the *S. nodorum* mutant strains *gna1-35*, *gba1-6* and *gga1-25* compared to the wild-type SN15, at near-sporulating$^{4°C}$ and sporulating$^{4°C}$ conditions are shown in Supplementary Tables 3 and 4. However it was the metabolites that were changing within the individual mutant strains during the transition to sporulation which was of most interest. These abundance changes are summarised in Tables 3 and 4. Generally, the abundance changes of most of the metabolites were comparable between mutants. Some of the more notable metabolite changes identified during cold-induced sporulation included the increase in abundance of putrescine, trehalose and octadecanoic acid in all of the mutants from both non-sporulating$^{22°C}$ or near-sporulating$^{4°C}$ conditions to sporulating$^{4°C}$. Surprisingly, mannitol levels decreased in each of the mutants during cold-induced differentiation as did the previously described metabolite

306 Unknown_35.27_2194_319 (IpCho *et al.*, 2010). The putative roles of these metabolites
307 are discussed in further detail below.
308

DISCUSSION

Glucose metabolism is altered in the *gna1, gba1* and *gga1* strains

After five days of growth, *S. nodorum* SN15 had a significantly higher amount of intracellular glucose than the mutant strains. The average abundance of glucose detected for SN15 was 4.6, 5.0 and 3.7 times more than observed for the *gna1-35*, *gba1-6* and *gga1-25* strains respectively. However, at this time point glucose still remained available in high abundance in the growth medium in both wild-type and mutant strains. By 10 days intracellular glucose levels had dropped dramatically, in some replicates to below detection limits, such that there was no significant difference between the amount of glucose within the mutants and wild-type. The large abundance of intracellular glucose observed in SN15 five dpi was not seen in any of the mutants under the conditions tested. As yet, extracellular glucose was still available at similar amounts in all strains, we conclude that the mutant strains may be further metabolizing the intracellular glucose rather than accumulating it like the wild-type.

The role of GPCRs and their associated G-proteins in nutrient sensing has been demonstrated in a number of fungal systems. Glucose sensing in *S. cerevisiae* for example has been shown to occur through the GPCR Gpr1. Glucose triggers an increase in cellular cAMP that is dependent on the Gα subunit (Gpa2) of the coupled heterotrimeric G-protein, which begins a protein kinase A (PKA)-mediated cascade of protein phosphorylation (Kraakman *et al.*, 1999). Here, the inactivation of *Gna1*, *Gba1* or *Gga1* alters glucose metabolism, possibly a result of a defect in detecting the nutrient levels available to the fungus, where the fate of glucose within the cell is changed.

Li et al. (2006) have also investigated the role of G-protein signalling on carbon source-dependent growth in *Neurospora crassa*. They demonstrated a critical role for GNA-1 (Class I Gα subunit) signalling in responding to different carbon sources by assessing the growth of an *N. crassa* mutants lacking either the G-protein coupled receptor GPR-4 or GNA-1. Interestingly, growth on glucose was relatively unaffected compared to growth on either glycerol or mannitol but this phenotype could be partially complemented by the exogenous application of cAMP.

There are multiple metabolic perturbations in the *gna1*, *gba1* and *ggaA* strains

The analysis of the primary metabolite abundances at five and 10 dpi highlighted the significant effect on metabolism caused by the inactivation of *Gna1*, *Gba1* and *Gga1.* Consistent with the deletion of the individual G-protein subunits of *A. nidulans* (Lafon *et al.*, 2005) and other fungal systems (Kraakman *et al.*, 1999) is an effect on the disaccharide trehalose. The decline in intracellular and extracellular glucose 10 dpi coincides with a dramatic increase in trehalose within the *S. nodorum* wild-type strain. Within the mutant strains, no significant change in trehalose abundance occurs between five and 10 dpi. insight into sexual development The accumulation of this metabolite has previously been correlated with asexual sporulation in *S. nodorum* both *in vitro* and *in planta* (Lowe *et al.*, 2009). Therefore, constitutive catabolism of trehalose in *S. nodorum* is consistent with the inability of the mutant strains *gna1-35*, *gba1-6* and *gga1-25* to sporulate under these experimental conditions, as trehalose is important for the growth and development of eukaryotic cells (Lowe *et al.*, 2009; Wilson *et al.*, 2007).

Constitutive catabolism of trehalose in *gna1-35*, *gba1-6* and *gga1-25* might also explain the reduced accumulation of glucose. In SN15 the depletion of intracellular glucose coincides with an accumulation of trehalose. It therefore appears that trehalose acts as a sink for excess glucose. Lafon *et al*., (2005) also observed the (albeit less significant, but) reduced catabolism of trehalose in the *sfa*D and *gpg*A strains of *A. nidulans*. This implies a role for all three G-protein subunits in trehalose degradation, and supports a similar requirement for Gna1, Gba1 and Gga1 in *S. nodorum*.

In wild-type, the drop in glucose abundance at 10 days of growth also coincides with a reduction in intracellular mannitol. The same trend was observed in *gba1-6*, but not for *gna1-35* or *gga1-25*. The latter two did not change significantly between five and 10 days, with mannitol remaining at a higher abundance. The abundance of mannitol observed in the combined intra/extracellular metabolite extracts between five and 10 days however does not change significantly in wild-type. But with intracellular mannitol showing a reduction, it is suggested that mannitol was being secreted by SN15 and *gba*1-6. Likewise, the intracellular mannitol pool of *gga*1-25 changed insignificantly over the growth period, yet when comparing the intra/extracellular amount, there was a significant ($p > 0.05$) increase in mannitol. This strain is therefore likely secreting excess mannitol into the growth medium.

Mannitol secretion has been reported in other phytophathogenic species including *Alternaria alternata*, and is believed to play a role in quenching the reactive oxygen species of the plant defence response (Jennings *et al.*, 1998; Jennings *et al.*, 2002). This is the first reported evidence of mannitol secretion by *S. nodorum*.

Changes to mannitol metabolism in the *gna*1 strain are also consistent with reports by (Casey *et al.*, 2010) which found mannitol dehydrogenase (Mdh1) to be the most up-

regulated protein in the *S. nodorum* mutant *gna1-35* strain when compared to the wild-type SN15, whilst mannitol 1-phosphate dehydrogenase (Mpd1) was significantly down-regulated. This metabolomic analysis further supports a role for Gna1, as well as Gba1 and Gga1, in regulating mannitol metabolism in *S. nodorum*, although its exact function is as yet unclear.

The disaccharide lactose was more abundant in the *S. nodorum* mutant strains compared to the wild-type. The metabolism of lactose is of emerging interest in *S. nodorum*. In the ascomycete *Hypocrea jecorina,* as with some other dissacharides, lactose can induce cellulase formation. Lactose has also shown this induction in *Acremonium cellulolyticus* (Fang et al., 2008) and in *Trichoderma reesei*, where lactose has been demonstrated to increase the expression of a number of cellulose-degrading enzymes (Foreman et al., 2003). *A. niger* on the other hand is unable to metabolise lactose (Seiboth *et al.*, 2007). The *S. nodorum* genome encodes the necessary enzymes for lactose degradation, although the biochemical pathway consists of a number of low specificity enzymes. Importantly however, as previously demonstrated, *S. nodorum* can utilise lactose as a sole carbon source (Gummer *et al.*, 2012). The slower growth of the *gga1-25* strain on lactose combined with the increased accumulation of this metabolite when grown on glucose, suggests that lactose is geared towards anabolism in *S. nodorum gga1-25*, as may be the case with a number of the *gga1* metabolites.

Dissecting the cold-induced sporulation phenomenom

We have recently showed that the prolonged incubation of the G-protein signalling mutants at 4°C complemented the sporulation defect. This observation provides a

401 unique opportunity to study the metabolome of *S. nodorum* as it differentiates from a
402 mature non-sporulating culture to an asexually sporulating culture.

403 A number of metabolites followed a pattern of increasing abundance in the metabolome
404 after three weeks (in the near-sporulating$^{4°C}$ conditions), but within six weeks under
405 these conditions (sporulating$^{4°C}$), the same metabolites depleted to within a similar
406 range as those 10 dpi (non-sporulating$^{22°C}$). These metabolites are believed to have
407 been induced by the cold-stress, rather than linked specifically to sporulation events,
408 and likely depleted upon starvation, following depletion of the carbon source by six
409 weeks at the cooler temperature. The change in these metabolites also followed a
410 similar pattern of abundance in the wild-type strain SN15.

411 The sugar-alcohol arabitol increased in abundance when the cultures were subjected to
412 three weeks growth at 4°C. The maximum abundance for this metabolite across all of
413 the culture conditions was also recorded under the near-sporulating$^{4°C}$ conditions, and
414 again in the *gga1-25* strain. As one of the four most abundant metabolites in *S. nodorum*,
415 arabitol was previously investigated and determined to play an osmoprotective role
416 within *S. nodorum* (Lowe *et al.*, 2008). This study now suggests that this polyol may also
417 play a role in the cold-stress tolerance of *S. nodorum*.

418 Another interesting molecule observed during the course of this study was alternariol.
419 Alternariol is a mycotoxin and of considerable interest due to the implications it poses
420 to human health, by exposure through crop contamination (Tan *et al.*, 2009b). It is
421 therefore of significant interest that the increased abundance of this secondary
422 metabolite is also found in the near-sporulating$^{4°C}$, cold-stressed strains. The maximum
423 abundance was detected in the wild-type strain SN15. The dramatic depletion of
424 intracellular alternariol from near-sporulating$^{4°C}$, to the sporulating$^{4°C}$ cultures of SN15,

where it was undetected, is also of interest. Previous studies on sporulation-impaired mutants of *S. nodorum* have previously linked alternariol and sporulation and further studies are now required to understand the role of this mycotoxin during differentiation (IpCho *et al.*, 2010).

The comparison of the non-sporulating metabolomes of the *S. nodorum gna1-35*, *gba1-6* and *gga1-25* strains with those extracted from the sporulation$^{4°C}$ cultures identified a number of metabolites correlating with the onset of sporulation. Some of the metabolites, although following a similar depletion in the transition from the non-sporulating$^{22°C}$ to the sporulating$^{4°C}$, were considered to have changed as a result of their relationship to glucose abundance. Fumarate, malate, fructose and mannitol were among these, and not believed direct 'markers' of either phenotype.

Putrescine was detected in all cold-induced sporulating mutant strains. Because this metabolite is also present in the comparable cultures of SN15, it is unlikely to be specifically associated with sporulation. Putrescine in *S. nodorum* is derived from the biochemical synthesis and degradation of arginine, all of the enzymes for which *S. nodorum* possesses. The disruption of some of the key enzymes of this pathway in *S. nodorum* may provide further insight into asexual development. Ornithine decarboxylase has been previously disrupted in *S. nodorum*. Whilst a reduction in pathogenicity was identified in the mutants, it was unclear whether or not the mutation affected sporulation (Bailey *et al.*, 2000).

The biochemical pathways of amine and polyamine degradation are used to derive nutrition from existing metabolites (Caspi *et al.*, 2008). The biochemical process of allantoin degradation forms one of these pathways and genomic evidence suggests that allantoin can be degraded to ureidoglycolate (urea producing) in *S. nodorum*. Allantoin

was significantly more abundant in the mutant strains five dpi, and by 10 dpi had accumulated to 8.6, 10.1, and 5.0 times higher abundance in *gna1-35*, *gba1-6* and *gga1-25*, compared to wild-type, respectively. The data suggests either an increased rate of urate degradation to allantoin in the mutant strains, or the reduced consumption/degradation of allantoin. Both options indicate likely differences in the nitrogen requirements of the mutant strains compared to the wild-type. In near-sporulating$^{4°C}$ cultures, the abundance of allantoin was reduced in the mutant strains, such that it was no longer significantly different to wild-type. In all strains, in the transition from the chilled near-sporulating$^{4°C}$ phenotype, to the sporulating$^{4°C}$, allantoin again increased in abundance.

The abundance of trehalose in these strains did not change significantly in the transition of the non-sporulating$^{22°C}$ phenotype to the near-sporulating$^{4°C}$. The abundance of this metabolite was therefore not correlated with the cold temperature. Just prior to sporulation (near-sporulating$^{4°C}$) the *gna*1, *gba*1 and *gga*A strains were significantly lower in trehalose abundance than the sporulating (sporulating$^{4°C}$) cultures. In the differentiation of this non-sporulating phenotype to that of a sporulating phenotype, trehalose increased 1.8, 4.0 and 3.7 fold in *gna1-35*, *gba1-6* and *gga1-25* respectively. Considering the huge natural abundance of trehalose in *S. nodorum*, these fold changes in abundance are noteworthy. The result conclusively supports the results of Lowe *et al*. (2009) in finding that the accumulation of trehalose is correlated with asexual sporulation in *S. nodorum*.

Of further interest in this dataset are the unidentified metabolites unknown_35.27_2194_319, and unknown_52.11_3560_307. Unknown_35.27_2194_319 is a metabolite that was found common to metabolite extracts of the non-sporulating

mutant strains *gna1-35*, *gba1-6* and *gga1-25*, but not the wild-type SN15 and therefore will likely play a role in asexual sporulation, perhaps as an inhibitor, or providing a necessary precursor for sporulation events. It is also interesting to note that Unknown_35.27_2194_319 was previously detected in *S. nodorum* SN15 following the first days of pycnidia development (5 dpi), however by 10 dpi when sporulation was rampant in SN15, the metabolite was completely absent from the SN15 metabolome, whilst remaining in the non-sporulating mutants under the equivalent growth conditions.

Conversely to Unknown_35.27_2194_319, Unknown_52.11_3560_307 is a metabolite common to metabolite extracts of *S. nodorum* SN15, but not of the mutant strains during sporulation. Although it was previously detected in *gna1-35* and *gga1-25* when not undergoing sporulation, this metabolite was significantly depleted compared to the asexually sporulating wild-type SN15 under the same growth conditions. This provides evidence that this metabolite is likely a biological 'marker' for the onset of asexual sporulation in *S. nodorum*. Further experimentation is required to elucidate the identity of these metabolites, which will inevitably help further dissect the lifecycle of *S. nodorum* and in particular, asexual sporulation.

Comparative analysis of the metabolome and proteome of the *S. nodorum gna1-35* strain

It is interesting to note the biochemical 'intersection' of glucose 6-phosphate in *S. nodorum*. Casey *et al.* (2010) observed differentially up and down-regulated enzymes involving glucose 6-phosphate, between the *S. nodorum gna1-35* mutant and the wild-type SN15, including glucose 6-phosphate 1-dehydrogenase, phosphoglucomutase and

497 inositol 3-phosphate synthase. Glucose 6-phosphate 1-dehydrogenase provides glucose
498 6-phosphate to the pentose phosphate pathway (PPP) and together with the
499 observation of the up-regulation of a number of enzymes of the PPP in *gna1-35*, it was
500 concluded that Gna1 signalling has an important regulatory role in determining the fate
501 of glucose 6-phosphate within *S. nodorum* (Casey *et al.*, 2010).

502 Further to this, the up-regulation of the PPP in *gna1-35* could be consequential or the
503 reason for the mutant strains' reduced growth rates and inability to form pycnidia
504 under these experimental conditions. With one of the primary objectives of the PPP
505 being to supply growing cells with pentose for the synthesis of nucleotides, from ribose
506 5-phosphate, this thesis further supports the conclusion by Casey *et al*. 2010.

507 In the *gna*1, *gba*1 and *gga*A strains at 5 dpi, there is evidence to suggest rather than
508 converting glucose 6-phosphate to fructose 6-phosphate (EC 2.7.1.1; ATP + D-Glucose
509 <=> ADP + D-Glucose 6-phosphate) and committing it to glycolysis by further
510 phosphorylation to fructose 1,6-bisphosphate (EC 2.7.1.11; ATP + D-fructose 6-
511 phosphate = ADP + D-fructose 1,6-bisphosphate), there is a preference for conversion of
512 glucose 6-phosphate to other sugar phosphates. The regulation would likely be
513 occurring through the allosteric inhibition of phosphofructokinase (PFK: EC; 2.7.1.11).
514 The inhibition maybe caused by the higher abundance of citrate in these strains
515 comparative to SN15, resulting in an increased abundance of myo-inositol at this earlier
516 time. This accumulation is supported by the observed up-regulation of inositol 3-
517 phosphate synthase in *gna*1, comparative to SN15 (Casey *et al.*, 2010).

518 With the aforementioned changes to glucose metabolism in the mutant strains, and as
519 glucose 6-phosphate provides a precursor requiring only two to three enzymatic

520 reactions to form mannitol, trehalose or myo-inositol (Figure 5), the metabolomic data
521 also supports a regulatory role for Gna1 in the fate of glucose 6-phosphate.
522

ACKNOWLEDGEMENTS

The authors would like to acknowledge the Grains Research and Development Corporation for its support. PSS is funded by an Australian Research Council Future Fellowship. The RUBY script was kindly provided by Robert Syme.

REFERENCES

Bailey, A., Mueller, E. & Bowyer, P. (2000). Ornithine decarboxylase of *Stagonospora* (*Septoria*) *nodorum* is required for virulence toward wheat. *J Biol Chem* **275**, 14242-14247.

Bringans, S., Hane, J. K., Casey, T., Tan, K. C., Lipscombe, R., Solomon, P. S. & Oliver, R. P. (2009). Deep proteogenomics; high throughput gene validation by multidimensional liquid chromatography and mass spectrometry of proteins from the fungal wheat pathogen *Stagonospora nodorum*. *BMC Bioinformatics* **10**, 301.

Casey, T., Solomon, P. S., Bringans, S., Tan, K.-C., Oliver, R. P. & Lipscombe, R. (2010). Quantitative proteomic analysis of G-protein signalling in *Stagonospora nodorum* using isobaric tags for relative and absolute quantification. *Proteomics* **10**, 38-47.

Caspi, R., Foerster, H., Fulcher, C. A. & other authors (2008). The MetaCyc Database of metabolic pathways and enzymes and the BioCyc collection of pathway/genome databases. *Nucleic Acids Research* **36**, D623-D631.

D'Enfert, C. (1997). Fungal spore germination: Insights from the molecular genetics of *Aspergillus nidulans* and *Neurospora crassa*. *Fungal Genet Biol* **21**, 163-172.

Fillinger, S., Chaveroche, M. K., van Dijck, P., de Vries, R., Ruijter, G., Thevelein, J. & d'Enfert, C. (2001). Trehalose is required for the acquisition of tolerance to a variety of stresses in the filamentous fungus *Aspergillus nidulans*. *Microbiology* **147**, 1851-1862.

Gummer, J. P., Waters, O. D. C., Krill, C., Du Fall, L., Trengove, R. D., Oliver, R. P. & Solomon, P. S. (2011). Metabolomics Protocols for Filamentous Fungi. In *Methods in Molecular Biology*. Edited by M. Bolton & B. Thomma. New York: Humana Press.

Gummer, J. P. A., Trengove, R. D., Oliver, R. P. & Solomon, P. S. (2012). A comparative analysis of the heterotrimeric G-protein G-alpha, G-beta and G-gamma subunits in the wheat pathogen *Stagonospora nodorum*. *BMC Microbiol*, 131.

IpCho, S. V. S., Tan, K.-C., Koh, G., Gummer, J., Oliver, R. P., Trengove, R. D. & Solomon, P. S. (2010). The transcription factor StuA regulates central carbon metabolism, mycotoxin production, and effector gene expression in the wheat pathogen *Stagonospora nodorum*. *Eukaryot Cell* **9**, 1100-1108.

Jennings, D. B., Ehrenshaft, M., Mason Pharr, D. & Williamson, J. D. (1998). Roles for mannitol and mannitol dehydrogenase in active oxygen-mediated plant defense. *Proceedings of the National Academy of Sciences of the United States of America* **95**, 15129-15133.

572 **Jennings, D. B., Daub, M. E., Pharr, D. M. & Williamson, J. D. (2002).** Constitutive
573 expression of a celery mannitol dehydrogenase in tobacco enhances resistance to the
574 mannitol-secreting fungal pathogen *Alternaria alternata*. *Plant J* **32**, 41-49.

575

576 **Kim, J. D., Kaiser, K., Larive, C. K. & Borkovich, K. A. (2011).** Use of 1H nuclear
577 magnetic resonance to measure intracellular metabolite levels during growth and
578 asexual sporulation in *Neurospora crassa*. *Eukaryot Cell* **10**, 820-831.

579

580 **Kraakman, L., Lemaire, K., Ma, P., Teunlssen, A. W. R. H., Donaton, M. C. V., Van**
581 **Dijck, P., Winderickx, J., De Winde, J. H. & Thevelein, J. M. (1999).** A *Saccharomyces*
582 *cerevisiae* G-protein coupled receptor, Gpr1, is specifically required for glucose
583 activation of the cAMP pathway during the transition to growth on glucose. *Mol*
584 *Microbiol* **32**, 1002-1012.

585

586 **Lafon, A., Seo, J. A., Han, K. H., Yu, J. H. & D'Enfert, C. (2005).** The heterotrimeric G-
587 protein GanB()-SfaD(Œ≤)-GpgA(Œ≥) is a carbon source sensor involved in early cAMP-
588 dependent germination in Aspergillus nidulans. *Genetics* **171**, 71-80.

589

590 **Li, L. & Borkovich, K. A. (2006).** GPR-4 is a predicted G-protein-coupled receptor
591 required for carbon source-dependent asexual growth and development in *Neurospora*
592 *crassa*. *Eukaryot Cell* **5**, 1287-1300.

593

Lowe, R. G., Lord, M., Rybak, K., Trengove, R. D., Oliver, R. P. & Solomon, P. S. (2008). A metabolomic approach to dissecting osmotic stress in the wheat pathogen *Stagonospora nodorum*. *Fungal Genet Biol* **45**, 1479-1486.

Lowe, R. G. T., Lord, M., Rybak, K., Trengove, R. D., Oliver, R. P. & Solomon, P. S. (2009). Trehalose biosynthesis is involved in sporulation of *Stagonospora nodorum*. *Fungal Genet Biol* **46**, 381-389.

Oliver, R. P. & Solomon, P. S. (2010). New developments in pathogenicity and virulence of necrotrophs. *Curr Opin Plant Biol* **13**, 415-419.

Oliver, R. P., Friesen, T. L., Faris, J. D. & Solomon, P. S. (2012). *Stagonospora nodorum*: From Pathology to Genomics and Host Resistance. *Annu Rev Phytopathol* **50**, null.

Seiboth, B., Pakdaman, B. S., Hartl, L. & Kubicek, C. P. (2007). Lactose metabolism in filamentous fungi: how to deal with an unknown substrate. *Fungal Biology Reviews* **21**, 42-48.

Solomon, P. S., Tan, K. C., Sanchez, P., Cooper, R. M. & Oliver, R. P. (2004). The disruption of a Gα subunit sheds new light on the pathogenicity of *Stagonospora nodorum* on wheat. *Mol Plant-Microbe Interact* **17**, 456-466.

Solomon, P. S., Tan, K. C. & Oliver, R. P. (2005). Mannitol 1-phosphate metabolism is required for sporulation in planta of the wheat pathogen *Stagonospora nodorum*. *Mol Plant-Microbe Interact* **18**, 110-115.

Solomon, P. S., Lowe, R. G. T., Tan, K. C., Waters, O. D. C. & Oliver, R. P. (2006a). *Stagonospora nodorum*: Cause of stagonospora nodorum blotch of wheat. *Mol Plant Pathol* **7**, 147-156.

Solomon, P. S., Rybak, K., Trengove, R. D. & Oliver, R. P. (2006b). Investigating the role of calcium/calmodulin-dependent protein kinases in *Stagonospora nodorum*. *Mol Microbiol* **62**, 367-381.

Solomon, P. S., Waters, O. D. C., Jörgens, C. I., Lowe, R. G. T., Rechberger, J., Trengove, R. D. & Oliver, R. P. (2006c). Mannitol is required for asexual sporulation in the wheat pathogen *Stagonospora nodorum* (glume blotch). *Biochem J* **399**, 231-239.

Solomon, P. S., Waters, O. D. C. & Oliver, R. P. (2007). Decoding the mannitol enigma in filamentous fungi. *Trends Microbiol* **15**, 257-262.

Tan, K. C., Heazlewood, J. L., Millar, A. H., Thomson, G., Oliver, R. P. & Solomon, P. S. (2008). A signaling-regulated, short-chain dehydrogenase of *Stagonospora nodorum* regulates asexual development. *Eukaryot Cell* **7**, 1916-1929.

Tan, K. C., Heazlewood, J. L., Millar, A. H., Oliver, R. P. & Solomon, P. S. (2009a). Proteomic identification of extracellular proteins regulated by the Gna1 Gα subunit in *Stagonospora nodorum*. *Mycol Res* **113**, 523-531.

Tan, K. C., Trengove, R. D., Maker, G. L., Oliver, R. P. & Solomon, P. S. (2009b). Metabolite profiling identifies the mycotoxin alternariol in the pathogen *Stagonospora nodorum*. *Metabolomics* **5**, 330-335.

Wilson, R. A., Jenkinson, J. M., Gibson, R. P., Littlechild, J. A., Wang, Z. Y. & Talbot, N. J. (2007). Tps1 regulates the pentose phosphate pathway, nitrogen metabolism and fungal virulence. *EMBO J* **26**, 3673-3685.

FIGURE LEGENDS

Fig. 1. Normalized mean abundances (± STD)* of mannitol in *S. nodorum* wild-type strain SN15 (Sn) and mutant strains *gna1-35*, *gba1-6* and *gga1-25* at 5 and 10 dpi. *Separation of the circles represents statistically different ($p < 0.05$) group means as determined by Tukey-Kramer analysis.

Fig. 2. Normalized mean abundances* (± std) of glucose in *S. nodorum* wild-type strain SN15 (Sn) and mutant strains *gna1-35*, *gba1-6* and *gga1-25* at 5 and 10 dpi. *Separation of the circles represents statistically different ($p < 0.05$) group means as determined by Tukey-Kramer analysis.

Fig. 3. PCA Scores plot displaying the Scores calculated from the normalised metabolite abundances of *S. nodorum* mutant strains grown under non-sporulating and sporulating culture conditions. The mutant strains *gna1-35* (α), *gba1-6* (β) and *gga1-25* (γ) were compared when sporulating (black circle), near sporulating (white circle) and non-sporulating (open symbol). Wild-type strain SN15 (WT) sporulated under all conditions; the displayed symbols represent comparable culture conditions to those of the mutant strains.

Fig. 4. The calculated loadings values contributing to the projections of the *S. nodorum* metabolites from strains *gna1-35*, *gba1-6* and *gga1-25* of the PCA Scores in Fig. 3.

Fig. 5. A schematic biochemical pathway outlining the fate of glucose 6-phosphate as determined by Casey *et al*. 2010; with added detail of metabolite data from 10 dpi (this thesis). "+" and "-"-symbols indicate the relative enzyme and metabolite abundances of *S. nodorum* strain *gna1-35* comparative to wild-type SN15. 1. Phosphoglucomutase; 2. Glucose 6-phosphate 1-dehydrogenase; 3. Inositol 3-phosphate synthase; 4. Mannitol 1-phosphate dehydrogenase (Mpd1); 5. Mannitol dehydrogenase (Mdh1); 6. 6-Phosphogluconate dehydrogenase; 7. Transketolase; 8. Transaldolase; 9. 3-Deoxy-7-phosphoheptulonate synthase. Adapted from Casey *et al.* 2010.

Table 1. Normalised mean abundance (± STD)* of identified metabolites contributing to the differences between the metabolome's of *S. nodorum* SN15 and mutant strains *gna*1-35, *gba*1-6 and *gga*1-25 after 5 days of growth.

	SN15			*gna1-35*			*gba1-6*			*gga1-25*		
Metabolite ID	Mean	±	STD	Mean	±	STD	Mean	±	STD	Mean	±	STD
Lactic acid 2TMS_10.93_1060_147	2.85	±	0.5	**10**	**±**	**2.52**	4.41	±	2.52	**8**	**±**	**2.07**
L-Isoleucine 2TMS_17.29_1295_158	0	±	0	0.27	±	0.51	**0.83**	**±**	**0.51**	**0.92**	**±**	**0.19**
L-Proline 2TMS_17.41_1300_142	0	±	0	**2.86**	**±**	**1.1**	**3.35**	**±**	**1.1**	**3.22**	**±**	**0.54**
L-Glycine 3TMS_17.61_1308_174	0.77	±	0.13	**1.6**	**±**	**0.55**	**1.66**	**±**	**0.55**	**1.44**	**±**	**0.28**
Succinic acid 2TMS_17.89_1319_147	4.15	±	0.88	10	±	6.09	**11.71**	**±**	**6.09**	8.98	±	2.58
L-Threonine 3TMS_19.60_1387_218	1.57	±	0.39	2.25	±	1.38	**3.49**	**±**	**1.38**	2.46	±	0.64
L-Glutamic acid 3TMS_24.85_1623_246	3.42	±	0.78	6.45	±	3.91	**9.89**	**±**	**3.91**	**8.32**	**±**	**1.36**
L-Phenylalanine 2TMS_24.99_1630_218	0	±	0	0	±	0.25	**0.59**	**±**	**0.25**	0.26	±	0.25
Arabinose 4TMS_25.64_1663_103	5.09	±	1.23	**9.83**	**±**	**2.9**	6.87	±	2.9	8.49	±	1.77
L-Asparagine 3TMS_25.87_1674_116	0.93	±	1.2	**4.58**	**±**	**2.7**	**5.35**	**±**	**2.7**	**5.85**	**±**	**1.65**
D-(-)-Ribose 4TMS_25.97_1679_103	0.03	±	0.08	0.3	±	0.27	**0.38**	**±**	**0.27**	0.3	±	0.17
Arabitol 5TMS_26.75_1719_217	4.27	±	3.25	1.95	±	0.37	0.25	±	0.37	**4.74**	**±**	**2.61**
Ornithine 4TMS_28.66_1815_142	10	±	4.2	**1.09**	**±**	**0.38**	**0.27**	**±**	**0.38**	**4.79**	**±**	**0.63**
Citric acid 4TMS_28.70_1817_273	1.98	±	0.68	4.76	±	3.96	**6.23**	**±**	**3.96**	**10**	**±**	**2.74**
Allantoin 4TMS_29.92_1878_331	0.35	±	0.19	**1.93**	**±**	**0.91**	**3.65**	**±**	**0.91**	**3.4**	**±**	**0.3**
Glucose 5TMS_30.21_1884_319	10	±	2.47	**2.01**	**±**	**1.73**	**1.61**	**±**	**1.73**	**2.47**	**±**	**1.49**
Glucose 5TMS_30.39_1902_319	10	±	2.43	**2.35**	**±**	**1.02**	**2.39**	**±**	**1.02**	**2.86**	**±**	**0.61**
L-Lysine 4TMS_30.58_1913_174	2.29	±	0.69	2.69	±	1.57	2.39	±	1.57	**4.1**	**±**	**0.74**
Mannitol 6TMS_30.59_1914_319	7.52	±	0.86	8.21	±	0.94	7.45	±	0.94	**9.35**	**±**	**1.19**
L-Tyrosine 3TMS_30.91_1933_218	0.42	±	0.34	1.33	±	1.66	**3**	**±**	**1.66**	**2.28**	**±**	**0.78**
Glucopyranose 5TMS_31.49_1967_204	10	±	4.57	**3.32**	**±**	**1.67**	**2.48**	**±**	**1.67**	**3.42**	**±**	**3.98**
myo-inositol 6TMS_32.32_2017_318	0.82	±	0.14	2.1	±	1.91	**3.49**	**±**	**1.91**	**4.28**	**±**	**1.56**
Octadecanoic acid 1TMS_35.97_2243_117	3.35	±	1.11	4.19	±	4.15	**7.52**	**±**	**4.15**	**7.67**	**±**	**0.9**
Fructose 5TMS_29.77_1870_103	5.56	±	3.34	2.99	±	2.07	3.38	±	2.07	3.98	±	0.83
Lactose 8TMS_41.93_2670_204	0.13	±	0.16	0.06	±	0	0	±	0	**0.61**	**±**	**0.21**
Alternariol 3TMS_45.58_2959_459	0.38	±	0.26	0.28	±	0.25	0.23	±	0.25	**1.13**	**±**	**0.66**
Ergosterol_48.39_3199_363	0.35	±	0.34	**1.98**	**±**	**0.68**	**2.36**	**±**	**0.68**	**1.81**	**±**	**0.32**

* The displayed metabolites each showed statistically significant differences in abundance between SN15 and at least one of the mutant strains; identified in bold. Metabolite abundances were scaled according to the maximum recorded abundance for each metabolite, across all measured growth conditions, which was scaled to 10; underlined. Statistical significance (<0.05) was determined by Tukey-Kramer HSD.

Table 2. Normalised mean abundance (± STD)* of identified metabolites contributing to the differences between the metabolome's of *S. nodorum* SN15 and mutant strains *gna*1-35, *gba*1-6 and *gga*1-25 after 10 days of growth.

	SN15			*gna1-35*			*gba1-6*			*gga1-25*		
Metabolite ID	Mean		STD	Mean		STD	Mean		STD	Mean		STD
L-Valine 2TMS_15.21_1211_144	1.21	±	0.19	**2.46**	**±**	**0.49**	1.13	±	0.98	**4.03**	**±**	**0.66**
L-Serine 2TMS_16.38_1258_132	4.62	±	1.34	6.45	±	1.7	4.14	±	1.4	**8.95**	**±**	**3.01**
L-Isoleucine 2TMS_17.29_1295_158	1.14	±	0.23	0.69	±	0.55	**0.12**	**±**	**0.3**	1.15	±	0.62
L-Proline 2TMS_17.41_1300_142	0.35	±	0.54	**4.11**	**±**	**0.98**	1.75	±	1.15	**4.61**	**±**	**3.14**
L-Glycine 3TMS_17.61_1308_174	1.06	±	0.22	**2.23**	**±**	**0.45**	0.82	±	0.34	**1.79**	**±**	**0.31**
Succinic acid 2TMS_17.89_1319_147	3.04	±	0.91	**3.12**	**±**	**0.73**	0.69	±	1.07	3.6	±	0.37
Fumaric acid 2TMS_18.89_1359_245	2.91	±	0.78	**8.5**	**±**	**2.88**	1.87	±	1.63	**10**	**±**	**1.36**
L-Alanine 3TMS_18.93_1361_188?	0	±	0	0	±	0	0	±	0	**3.69**	**±**	**4.15**
L-Threonine 3TMS_19.60_1387_218	2.21	±	0.46	**4.56**	**±**	**0.73**	**3.88**	**±**	**1.23**	3.18	±	1.43
Erythritol 4TMS_21.21_1492_217	0	±	0	**0.78**	**±**	**0.08**	0.19	±	0.29	**1.41**	**±**	**0.78**
Malic acid 3TMS_22.01_1484_147	3.72	±	0.8	**10**	**±**	**2.41**	3	±	2.83	**9.39**	**±**	**0.8**
2-Ketoglutaric acid 2TMS_24.04_1582	2.38	±	0.44	4.64	±	1.63	2.34	±	2.15	**7.93**	**±**	**2.96**
Tryptamine_24.44_1602_188	0.72	±	0.26	0.71	±	0.13	**1.36**	**±**	**0.46**	0.67	±	0.12
L-Phenylalanine 2TMS_24.99_1630_218	0.05	±	0.13	**0.81**	**±**	**0.16**	0.15	±	0.26	**0.47**	**±**	**0.38**
Arabitol 5TMS_26.75_1719_217	0.06	±	0.05	0.31	±	0.17	0.7	±	1.71	**4.47**	**±**	**1.41**
Citric acid 4TMS_28.70_1817_273	2.37	±	0.47	3.98	±	1.38	4.89	±	5.12	**8.3**	**±**	**1.02**
Fructose 5TMS_29.59_1861_103	0.07	±	0.17	0.79	±	0.18	0.4	±	0.99	**1.06**	**±**	**0.45**
Allantoin 4TMS_29.92_1878_331	0.99	±	0.68	**8.49**	**±**	**3.92**	**10**	**±**	**2.76**	4.92	±	2.87
Mannitol 6TMS_30.59_1914_319	2.69	±	0.7	**8.34**	**±**	**1.33**	2.42	±	3.36	**10**	**±**	**1.61**
L-Tyrosine 3TMS_30.91_1933_218	1.21	±	0.32	**3.58**	**±**	**0.73**	1.33	±	0.76	**2.63**	**±**	**1.32**
Gluconic acid 6TMS_31.82_1987_147	0.07	±	0.1	0.15	±	0.14	0	±	0	**0.37**	**±**	**0.11**
L-Glutamine 4TMS_31.95_1995_227	0	±	0	0	±	0	0	±	0	**10**	**±**	**11.25**
myo-inositol 6TMS_32.32_2017_318	10	±	1.28	**3.83**	**±**	**1.99**	**4.46**	**±**	**1.58**	**6.96**	**±**	**1.07**
Hexdecanoic acid 1TMS_32.83_2048_117	6.78	±	2.2	5.39	±	0.96	**3.24**	**±**	**0.69**	**4.5**	**±**	**0.91**
Octadecanoic acid 1TMS_35.97_2243_117	4.93	±	1.75	2.47	±	0.56	2.9	±	1	2.37	±	0.37
Fructose 5TMS_29.77_1870_103	0	±	0	0	±	0	0.34	±	0.84	0.7	±	0.41
Lactose 8TMS_41.93_2670_204	0	±	0	0	±	0	0.13	±	0.33	**0.73**	**±**	**0.43**
Trehalose 8TMS_42.69_2725_361	10	±	1.06	**0.16**	**±**	**0.1**	**0.28**	**±**	**0.49**	**1.02**	**±**	**0.32**
Alternariol 3TMS_45.58_2959_459	1.23	±	0.85	**0**	**±**	**0**	**0.13**	**±**	**0.11**	**0.03**	**±**	**0.07**
Ergosterol_48.39_3199_363	1.64	±	0.75	**5.56**	**±**	**1.07**	**6.12**	**±**	**2.15**	**4.59**	**±**	**0.63**

* The displayed metabolites each showed statistically significant differences in abundance between SN15 and at least one of the mutant strains; identified in bold. Metabolite abundances were scaled according to the maximum recorded abundance for each metabolite, across all measured growth conditions, which was scaled to 10; underlined. Statistical significance (<0.05) was determined by Tukey-Kramer HSD.

Table 3. The fold-change in metabolite abundance between cultures of *S. nodorum* strains *gna*1-35, *gba*1-6 and *gga*1-25 when grown under non-sporulating$^{22°C}$ conditions, compared to the same strain during sporulation$^{4°C}$ (6 weeks chilled at 4°C).

	Δ Abundance		
Metabolite ID	*gna*1-35	*gba*1-6	*gga*A-25
Fumaric acid 2TMS_18.89_1359_245	↓[1] 4.5	↓ 2.36	↓ 5.78
Malic acid 3TMS_22.01_1484_147	↓ 2.07	↓ 2.95	↓ 2.2
Arabinose 4TMS_25.64_1663_103	↓ ×[2]	×	↓ ×
Unknown_29.29_1846_285	↓ ×	×	↓ ×
Fructose 5TMS_29.59_1861_103	↓ 2.14	↓ 1.18	↓ 7.07
Allantoin 5TMS_29.79_1871_518?	↓ 1.26	↓ 1.68	↓ ×
Allantoin 4TMS_29.92_1878_331	↓ 2.88	↓ 3.98	↓ 1.11
Mannitol 6TMS_30.59_1914_319	↓ 1.96	↓ 1.09	↓ 4.22
Unknown_35.27_2194_319	↓ 63.5	↓ ×	↓ ×
Putrescine 3TMS_21.37_1458_174	↑ ×	↑ ×	↑ ×
Tryptamine_24.44_1602_188	↑ 11.97	↑ 7.35	↑ 7.36
Unknown_28.85_1824_231	↑ 2.14	↑ 3.63	↑ 1.89
Unknown_28.95_1829_147	↑ 1.86	↑ 2.25	↑ 1.22
Octadecanoic acid 1TMS_35.97_2243_117	↑ 2.47	↑ 3.45	↑ 3.81
Trehalose 8TMS_42.69_2725_361	1	↑ 1.57	↑ 1.24
Unknown_52.11_3560_307	↑ 8	↑ ×	↑ 10.76

[1] The arrows indicate whether the metabolite is increased or decreased in abundance under sporulating$^{4°C}$ compared to non-sporulating$^{22°C}$.

[2] The 'x' symbol indicates that the metabolite wasn't present in either the non-sporulating$^{22°C}$ or sporulating$^{4°C}$ samples.

Table 4. The fold-change in metabolite abundance between cultures of *S. nodorum* strains *gna*1-35, *gba*1-6 and *gga*1-25 when grown under near-sporulating$^{4°C}$ conditions (3 weeks chilled at 4°C), compared to the same strain when asexually sporulating$^{4°C}$ (6 weeks chilled at 4°C).

	Δ Abundance		
Metabolite ID	*gna*1-35	*gba*1-6	*gga*A-25
Arabinose 4TMS_25.64_1663_103	↓[1] ×[2]	↓ ×	↓ ×
Unknown_28.95_1829_147	↑ 1.47	↓ 1.21	↓ 1.9
Unknown_29.29_1846_285	↓ ×	↓ ×	1
Fructose 5TMS_29.59_1861_103	↓ 27.03	↓ 11.96	↓ 28.8
Mannitol 6TMS_30.59_1914_319	↓ 1.96	↓ 3.41	↓ 1.95
Unknown_35.27_2194_319	↓ ×	↓ ×	↓ ×
Fumaric acid 2TMS_18.89_1359_245	↑ 1.45	↑ 3.4	↑ 1.29
Putrescine 3TMS_21.37_1458_174?	↑ ×	↑ 37.04	↑ ×
Malic acid 3TMS_22.01_1484_147	↑ 1.16	↑ 1.8	↓ 1.12
Tryptamine_24.44_1602_188	↑ 26.56	↑ 17.54	↑ 6.94
Unknown_28.85_1824_231	↑ 7.3	↑ 10.03	↑ 5.84
Allantoin 5TMS_29.79_1871_518	↑ ×	↑ ×	↑ ×
Allantoin 4TMS_29.92_1878_331	↑ 5.46	↓ 1.06	↑ 1.09
Octadecanoic acid 1TMS_35.97_2243_117	↑ 4.76	↑ 6.13	↑ 3.47
Trehalose 8TMS_42.69_2725_361	↑ 1.78	↑ 4	↑ 3.71
Unknown_52.11_3560_307	↑ ×	↑ ×	↑ ×

[1] The arrows indicate whether the metabolite is increased or decreased in abundance under sporulating$^{4°C}$ compared to non-sporulating$^{22°C}$.

[2] The 'x' symbol indicates that the metabolite wasn't present in either the near-sporulating$^{22°C}$ or asexually sporulating$^{4°C}$ sample.

Fig. 1

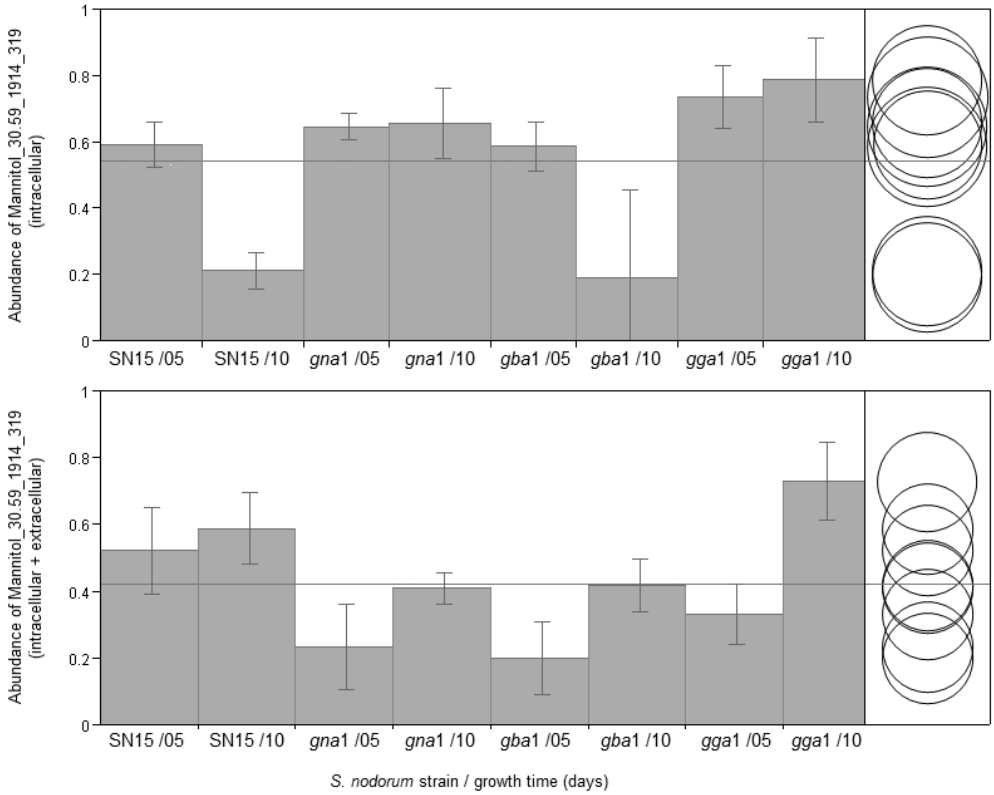
Abundance of Mannitol_30.59_1914_319 (intracellular)
1
0.8
0.6
0.4
0.2
0
SN15 /05
SN15 /10
gna1 /05
gna1 /10
gba1 /05
gba1 /10
gga1 /05
gga1 /10
Abundance of Mannitol_30.59_1914_319 (intracellular + extracellular)
S. nodorum strain / growth time (days)

Fig. 2

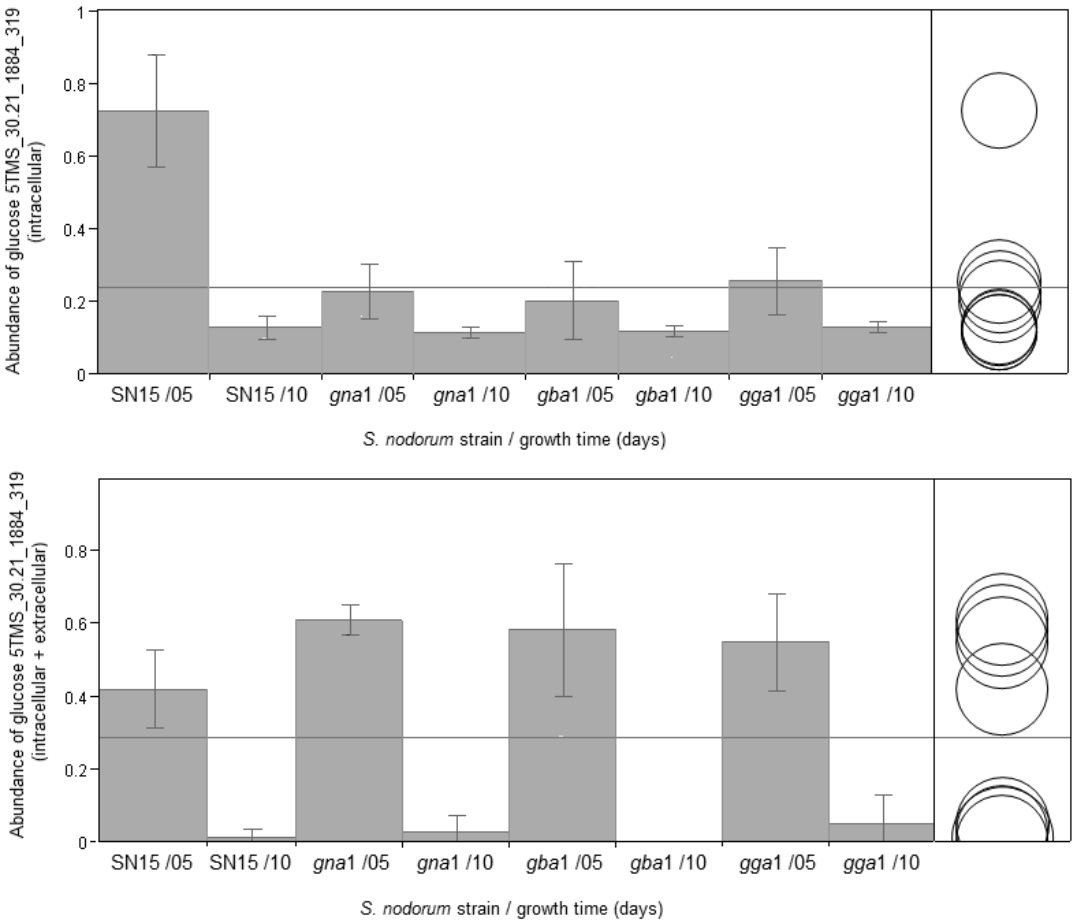
Abundance of glucose 5TMS_30.21_1884_319 (intracellular)
1
0.8
0.6
0.4
0.2
0
SN15 /05
SN15 /10
gna1 /05
gna1 /10
gba1 /05
gba1 /10
gga1 /05
gga1 /10
S. nodorum strain / growth time (days)
Abundance of glucose 5TMS_30.21_1884_319 (intracellular + extracellular)
0.8
0.6
0.4
0.2
0
SN15 /05
SN15 /10
gna1 /05
gna1 /10
gba1 /05
gba1 /10
gga1 /05
gga1 /10
S. nodorum strain / growth time (days)

Fig. 3

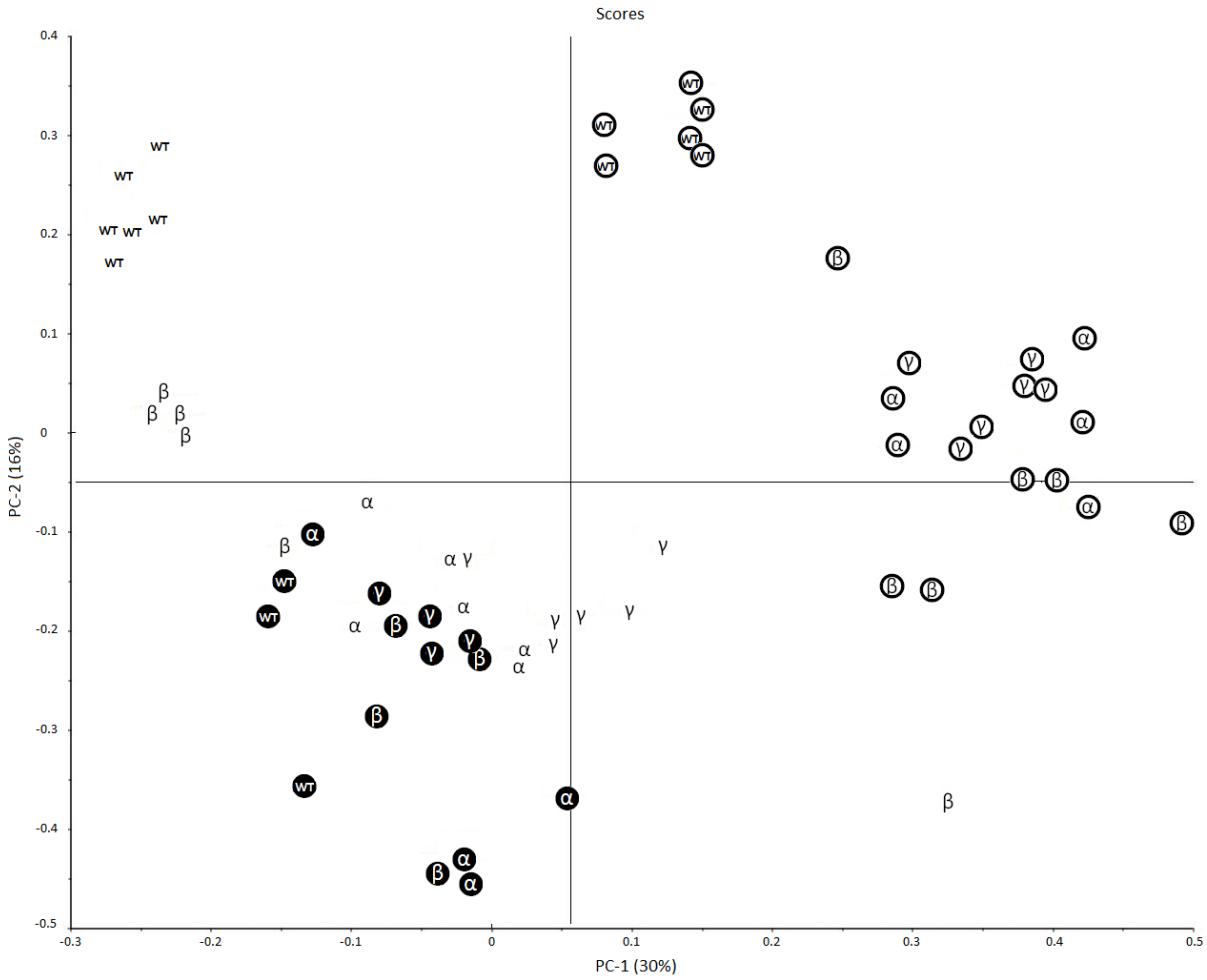

S. nodorum strain	Identifier	Culture conditions	Phenotype
wild-type SN15	WT	22°C 10 days	Sporulating
	Ⓦ	22°C/5 days ⟶ 4C°/3 weeks	Sporulating
	Ⓦ	22°C/5 days ⟶ 4C°/6 weeks	Sporulating
mutant *gna* 1-35	α	22°C 10 days	Non-sporulating
	Ⓐ	22°C/5 days ⟶ 4C°/3 weeks	Near sporulating
	Ⓐ	22°C/5 days ⟶ 4C°/6 weeks	Sporulating
mutant *gba* 1-6	β	22°C 10 days	Non-sporulating
	Ⓑ	22°C/5 days ⟶ 4C°/3 weeks	Near sporulating
	Ⓑ	22°C/5 days ⟶ 4C°/6 weeks	Sporulating
mutant *gga* 1-25	γ	22°C 10 days	Non-sporulating
	Ⓒ	22°C/5 days ⟶ 4C°/3 weeks	Near sporulating
	Ⓒ	22°C/5 days ⟶ 4C°/6 weeks	Sporulating

Fig. 4

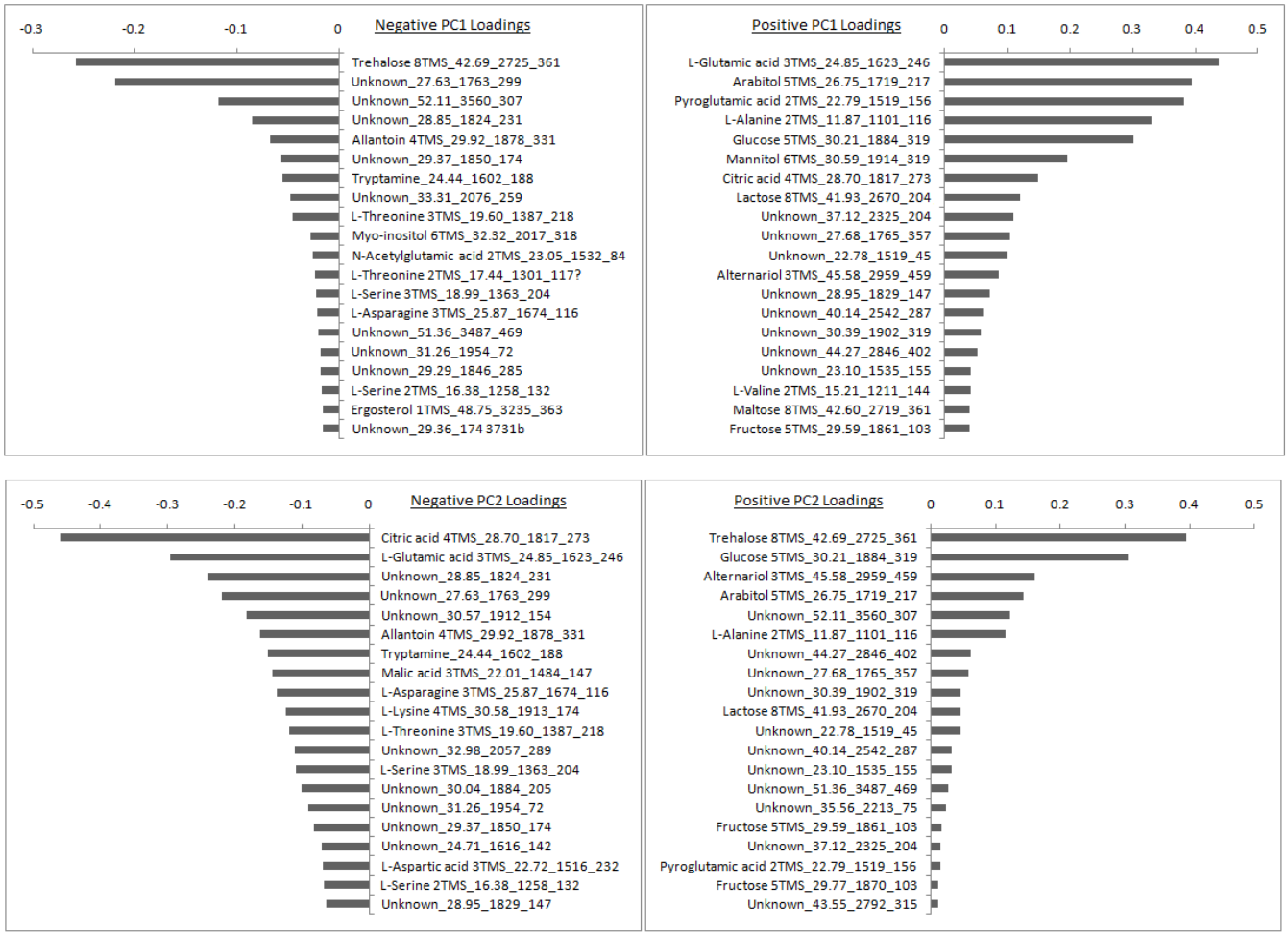
Negative PC1 Loadings
-0.3
-0.2
-0.1
0
Trehalose 8TMS_42.69_2725_361
Unknown_27.63_1763_299
Unknown_52.11_3560_307
Unknown_28.85_1824_231
Allantoin 4TMS_29.92_1878_331
Unknown_29.37_1850_174
Tryptamine_24.44_1602_188
Unknown_33.31_2076_259
L-Threonine 3TMS_19.60_1387_218
Myo-inositol 6TMS_32.32_2017_318
N-Acetylglutamic acid 2TMS_23.05_1532_84
L-Threonine 2TMS_17.44_1301_117?
L-Serine 3TMS_18.99_1363_204
L-Asparagine 3TMS_25.87_1674_116
Unknown_51.36_3487_469
Unknown_31.26_1954_72
Unknown_29.29_1846_285
L-Serine 2TMS_16.38_1258_132
Ergosterol 1TMS_48.75_3235_363
Unknown_29.36_174 3731b
Positive PC1 Loadings
0
0.1
0.2
0.3
0.4
0.5
L-Glutamic acid 3TMS_24.85_1623_246
Arabitol 5TMS_26.75_1719_217
Pyroglutamic acid 2TMS_22.79_1519_156
L-Alanine 2TMS_11.87_1101_116
Glucose 5TMS_30.21_1884_319
Mannitol 6TMS_30.59_1914_319
Citric acid 4TMS_28.70_1817_273
Lactose 8TMS_41.93_2670_204
Unknown_37.12_2325_204
Unknown_27.68_1765_357
Unknown_22.78_1519_45
Alternariol 3TMS_45.58_2959_459
Unknown_28.95_1829_147
Unknown_40.14_2542_287
Unknown_30.39_1902_319
Unknown_44.27_2846_402
Unknown_23.10_1535_155
L-Valine 2TMS_15.21_1211_144
Maltose 8TMS_42.60_2719_361
Fructose 5TMS_29.59_1861_103
Negative PC2 Loadings
-0.5
-0.4
-0.3
-0.2
-0.1
0
Citric acid 4TMS_28.70_1817_273
L-Glutamic acid 3TMS_24.85_1623_246
Unknown_28.85_1824_231
Unknown_27.63_1763_299
Unknown_30.57_1912_154
Allantoin 4TMS_29.92_1878_331
Tryptamine_24.44_1602_188
Malic acid 3TMS_22.01_1484_147
L-Asparagine 3TMS_25.87_1674_116
L-Lysine 4TMS_30.58_1913_174
L-Threonine 3TMS_19.60_1387_218
Unknown_32.98_2057_289
L-Serine 3TMS_18.99_1363_204
Unknown_30.04_1884_205
Unknown_31.26_1954_72
Unknown_29.37_1850_174
Unknown_24.71_1616_142
L-Aspartic acid 3TMS_22.72_1516_232
L-Serine 2TMS_16.38_1258_132
Unknown_28.95_1829_147
Positive PC2 Loadings
0
0.1
0.2
0.3
0.4
0.5
Trehalose 8TMS_42.69_2725_361
Glucose 5TMS_30.21_1884_319
Alternariol 3TMS_45.58_2959_459
Arabitol 5TMS_26.75_1719_217
Unknown_52.11_3560_307
L-Alanine 2TMS_11.87_1101_116
Unknown_44.27_2846_402
Unknown_27.68_1765_357
Unknown_30.39_1902_319
Lactose 8TMS_41.93_2670_204
Unknown_22.78_1519_45
Unknown_40.14_2542_287
Unknown_23.10_1535_155
Unknown_51.36_3487_469
Unknown_35.56_2213_75
Fructose 5TMS_29.59_1861_103
Unknown_37.12_2325_204
Pyroglutamic acid 2TMS_22.79_1519_156
Fructose 5TMS_29.77_1870_103
Unknown_43.55_2792_315

Fig. 5

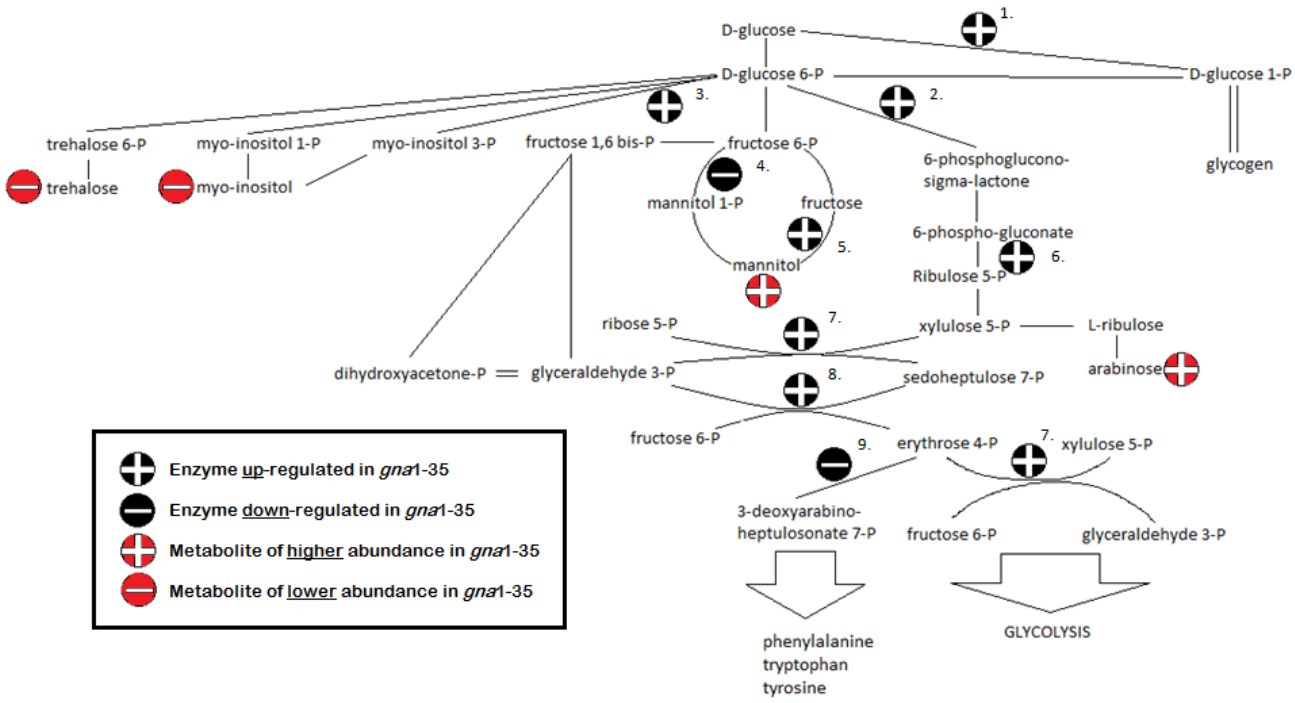
D-glucose
1.
D-glucose 6-P
D-glucose 1-P
2.
3.
trehalose 6-P
myo-inositol 1-P
myo-inositol 3-P
fructose 1,6 bis-P
fructose 6-P
6-phosphoglucono-
sigma-lactone
glycogen
trehalose
myo-inositol
4.
mannitol 1-P
fructose
5.
mannitol
6-phospho-gluconate
6.
Ribulose 5-P
ribose 5-P
7.
xylulose 5-P
L-ribulose
dihydroxyacetone-P
glyceraldehyde 3-P
8.
sedoheptulose 7-P
arabinose
fructose 6-P
9.
erythrose 4-P
7.
xylulose 5-P
3-deoxyarabino-
heptulosonate 7-P
fructose 6-P
glyceraldehyde 3-P
phenylalanine
tryptophan
tyrosine
GLYCOLYSIS
Enzyme up-regulated in gna1-35
Enzyme down-regulated in gna1-35
Metabolite of higher abundance in gna1-35
Metabolite of lower abundance in gna1-35